Operation of Brillouin Optical Correlation-Domain Reflectometry: Theoretical Analysis and Experimental Validation

Yosuke Mizuno, Weiwen Zou, *Member, IEEE, OSA*, Zuyuan He, *Member, IEEE, OSA*, and Kazuo Hotate, *Fellow, IEEE*

***Abstract*—We theoretically and experimentally analyze the operation of Brillouin optical correlation-domain reflectometry (BOCDR). First, we experimentally confirm that BOCDR is not based on stimulated Brillouin scattering but on spontaneous Brillouin scattering. Then, we theoretically prove that the spatial resolution of BOCDR is given well by the same expression as that of Brillouin optical correlation-domain analysis (BOCDA). Finally, we demonstrate that the modulation amplitude of the laser frequency, which has been conventionally limited to a half of the Brillouin frequency shift, can be enhanced further by employing a sensing fiber shorter than a half of the measurement range.**

***Index Terms*—Brillouin scattering, correlation, distributed measurement, modulation, nonlinear optics, reflectometry.**

I. Introduction

BRILLOUIN scattering-based fiber-optic sensors have been widely studied as a promising technology for monitoring conditions in various materials and structures, due to their capability of a distributed measurement of strain and/or temperature along a fiber under test (FUT). Above all, the following three techniques have been extensively studied: Brillouin optical time-domain reflectometry (BOTDR) [1], [3], [4], Brillouin optical time-domain analysis (BOTDA) [5]–[11], and Brillouin optical correlation-domain analysis (BOCDA) [12]–[15]. BOTDR and BOTDA have the measurement range as long as several tens of kilometers, and BOCDA has an extremely high spatial resolution ($\sim$1.6 mm [14]). However, the inherent limitation of the spatial resolution in basic time-domain techniques is about 1 m [16], [17], though several methods have recently been developed to enhance the resolution [4], [8]–[11]. Meanwhile, in standard BOCDA, two lightwaves must be injected into both ends of the FUT. Even in the linear configuration of BOCDA [15], where a mirror is employed at one end of the FUT, if part of the FUT cracks, the distributed measurement can no longer be performed.

In order to achieve a high spatial resolution and substantial one-end accessibility simultaneously, we have proposed Brillouin optical correlation-domain reflectometry (BOCDR) [18], which is based on the correlation control of continuous lightwaves. So far, 13-mm spatial resolution has been obtained for a silica fiber [19]. By using a tellurite glass fiber as the FUT, 6-mm resolution has also been achieved [20].

It has been assumed that BOCDR is based on spontaneous Brillouin scattering, not on stimulated Brillouin scattering (SBS). However, it was not clarified yet. On the other hand, the expression for the spatial resolution in BOCDR has been assumed to be the same as that in BOCDA [18], but this was not theoretically proved yet. Furthermore, the modulation amplitude and the modulation frequency of the laser frequency must be increased to achieve a high spatial resolution, but their theoretical limitations were not clarified yet.

In this paper, first, we experimentally show that BOCDR is not based on SBS but on spontaneous Brillouin scattering. Next, we describe that BOCDA and BOCDR are based on quite different operating principles, and that the operation of BOCDR should be analyzed independently of that of BOCDA. Then, we theoretically show that the spatial resolution of BOCDR is given well by the same expression as that of BOCDA, and clarify the theoretical limitation of the modulation frequency. Finally, we analyze the Rayleigh scattering-induced noise, and theoretically and experimentally clarify the limitation of the modulation amplitude.

II. Proof That BOCDR Is Based on Spontaneous Brillouin Scattering

If the power of the incident light is extremely high, SBS is observed even when the light is injected into only one end of the fiber. This is because the backscattered Stokes light due to spontaneous Brillouin scattering works as a probe lightwave in SBS. In this section, we experimentally clarified that SBS is not dominant in BOCDR.

Manuscript received July 27, 2010; revised September 13, 2010; accepted September 20, 2010. Date of publication September 27, 2010; date of current version November 17, 2010. This work was supported in part by the Grant-in-Aid for Scientific Research (S) and the Global Center of Excellence (G-COE) Program from the Ministry of Education, Culture, Sports, Science and Technology (MEXT), Japan. The work of Y. Mizuno was supported by the Research Fellowships for Young Scientists from the Japan Society for the Promotion of Science (JSPS).

Y. Mizuno was with the Department of Electrical Engineering and Information Systems, The University of Tokyo, Tokyo 113-8656, Japan. He is now with Precision and Intelligence Laboratory, Tokyo Institute of Technology, Kanagawa 226-8503, Japan (e-mail: ymizuno@sonic.pi.titech.ac.jp).

W. Zou was with the Department of Electrical Engineering and Information Systems, The University of Tokyo, Tokyo 113-8656, Japan. He is now with the Department of Electronic Engineering, Shanghai Jiao Tong University, Shanghai 200240, China (e-mail: wzou@sjtu.edu.cn).

Z. He and K. Hotate are with the Department of Electrical Engineering and Information Systems, The University of Tokyo, Tokyo 113-8656, Japan (e-mail: ka@sagnac.t.u-tokyo.ac.jp; hotate@sagnac.t.u-tokyo.ac.jp).

Color versions of one or more of the figures in this paper are available online at http://ieeexplore.ieee.org.

Digital Object Identifier 10.1109/JLT.2010.2081348

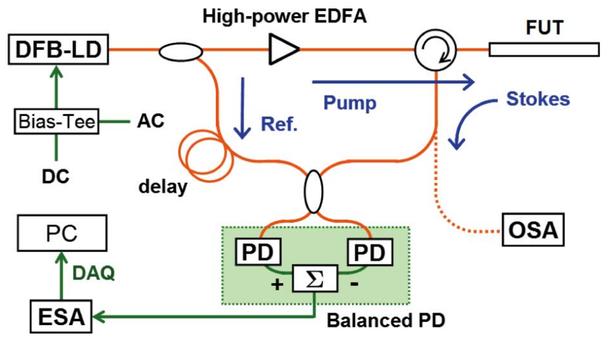

Fig. 1. Conceptual setup of the basic BOCDR system. The OSA is used to directly observe the Stokes light spectrum. AC, alternating current; DAQ, data acquisition; DC, direct current; DFB-LD, distributed-feedback laser diode; EDFA, erbium- doped fiber amplifier; ESA, electrical spectrum analyzer; FUT, fiber under test; OSA, optical spectrum analyzer; PC, personal computer; PD, photodetector.

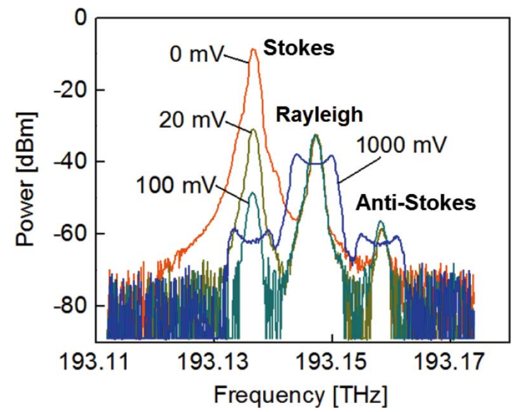

Fig. 2. Measured optical spectra of the reflected light.

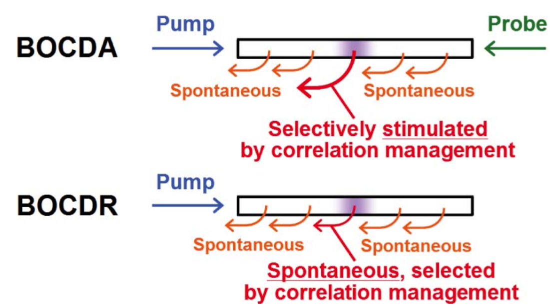

Fig. 3. Principles of BOCDA and BOCDR.

Fig. 1 depicts the schematic drawing of the BOCDR system [18]. Spontaneous Brillouin scattering caused in the FUT makes interference with the reference lightwave, which is detected with balanced photo-detectors (PDs). By modulating the laser frequency with a sinusoidal waveform, a correlation peak is synthesized at one point along the FUT [18]. In the experiment to confirm that the Brillouin scattering caused in the FUT of BOCDR is spontaneous one, the reference path was removed in Fig. 1, and an optical spectrum analyzer (OSA) was employed to observe the backscattered Stokes light. The frequency-modulated light beam from a distributed-feedback laser diode (DFB-LD) at 1550 nm was amplified up to 28 dBm with an erbium-doped fiber amplifier (EDFA), and was injected into a 1-km FUT. The modulation frequency of the laser frequency $f_{\rm m}$ was fixed at 68.62 kHz. Since it is difficult to accurately measure the modulation amplitude Δf because of the limited resolution of the OSA, the peak-to-peak output voltage of the function generator (FG) providing alternating current (AC) to the DFB-LD was substituted for Δf, and it was set to 0, 20, 100, and 1000 $\mathrm{mV_{pp}}$.

Fig. 2 shows the measured optical spectra of the Stokes light when Δf was increased. With no modulation applied ($\Delta f = 0$ GHz), the power of the Stokes light is higher than that of the Rayleigh-scattered light by more than 20 dB, which indicates the presence of SBS. However, as Δf was increased, the power of the Stokes light drastically decreased; when the AC was 1000 $\mathrm{mV_{pp}}$ corresponding to Δf of about 3 GHz, it was lower than the power of the Rayleigh-scattered light by about 20 dB. This change in the power of the Stokes light seems to be caused by the transition from SBS to spontaneous Brillouin scattering. Since Δf in BOCDR is generally set to several GHz [18], it was clarified that BOCDR is based not on SBS but on spontaneous Brillouin scattering. Therefore, the Brillouin signal of BOCDR is expected to be weaker than those of SBS-based techniques such as BOTDA and BOCDA.

III. Comparison Between BOCDA and BOCDR

We compare the operating principles between the two correlation-domain techniques: two-end-access BOCDA [12] and one-end-access BOCDR [18]. As shown in Fig. 3, in both systems, the pump light is reflected everywhere in the FUT due to spontaneous Brillouin scattering. In order to resolve the position, in BOCDA, SBS is induced selectively at one specific position in the FUT by injecting the frequency-modulated, or correlation-managed, pump and probe light beams into each end of the FUT. Strictly speaking, the effective Brillouin gain spectrum (BGS) obtained in BOCDA is built up of the sum of the Brillouin signals at all the positions along the FUT, and only the Brillouin signal at the correlation peak is sharp and contributes to the effective BGS, while the Brillouin signals at other sections spread out [12]. In contrast, in BOCDR, the Stokes light due to spontaneous Brillouin scattering from one specific position in the FUT is selectively observed by the heterodyne detection with the frequency-modulated, or correlation-managed, reference light (See Fig. 1). Thus, BOCDA and BOCDR are based on quite different operating principles, so we need to analyze the operation of BOCDR independently of that of BOCDA.

IV. Theoretical Analysis of BOCDR Operation

A. System Formulation

First, we derive the expression of the effective BGS, which is the final signal observed with the electrical spectrum analyzer (ESA) in BOCDR. We define the position of the correlation peak in the FUT as $z = z_{\rm m}$, which corresponds to the measuring position. Suppose the electric field spectra of the reference light, the pump light (per unit length), and the Stokes light (per unit length) are $\tilde{E}_{\rm r}(f)(= F\{E_{\rm r}(t)\})$, $\tilde{E}_{\rm p}(z - z_{\rm m}, f)(= F\{E_{\rm p}(z - z_{\rm m}, t)\})$, and $\tilde{E}_{\rm S}(z{-}z_{\rm m}, f)(= F\{E_{\rm S}(z{-}z_{\rm m}, t)\})$, respectively. Here $F\{\cdot\}$ denotes the operation of Fourier transform. Then, as shown in Fig. 4, $\tilde{E}_{\mathrm{S}}(z-z_m,f)$ is approximately expressed as (See Appendix)

$$\begin{aligned}\tilde{E}_S(z-z_m,f) &= \tilde{E}_p(z-z_m,f+f_B(z))\otimes_f \tilde{D}(z,f)\\ &\equiv \tilde{E}'_S(z-z_m,f)\otimes_f \tilde{D}(z,f),\end{aligned} \tag{1}$$

where $f_{\mathrm{B}}(z)$ is the Brillouin frequency shift (BFS), $\otimes_f$ represents a convolution concerning frequency, and $\tilde{D}(z,f)(=\ F\{D(z,t)\})$ is a complex Lorentzian function given by

$$\tilde{D}(z,f)=\frac{g_{B0}^{1/2}}{1-j2f/\Delta\nu_B}, \tag{2}$$

where g_{B0} is the Brillouin gain coefficient, and $\Delta\nu_{\mathrm{B}}$ is the Brillouin bandwidth. The Stokes light generated along the whole length of the FUT is given as

$$\int_{\mathrm{FUT}} dz\cdot E_S(z-z_m,t), \tag{3}$$

and the total electric field on the detector is expressed as

$$E_r(t)+\int_{\mathrm{FUT}} dz\cdot E_S(z-z_m,t). \tag{4}$$

Then, the interference signal $I(z_{\mathrm{m}},t)$ between the Stokes light and the reference light is given as

$$I(z_m,t)\propto\left\langle\left|E_r(t)+\int_{\mathrm{FUT}} dz\cdot E_S(z-z_m,t)\right|^2\right\rangle, \tag{5}$$

where $\langle\cdot\rangle$ stands for time-averaging operation, and its AC component around the BFS is

$$\begin{aligned}&I_{\mathrm{AC}}(z_m,t)\\ &\quad\propto\int_{\mathrm{FUT}} dz\cdot\langle E_r^*(t)E_S(z-z_m,t)+c.c.\rangle\\ &\quad=\int_{\mathrm{FUT}} dz\cdot\left\langle E_r^*(t)E_S^{'}(z-z_m,t)D(z,t)+c.c.\right\rangle\end{aligned} \tag{6}$$

where c.c. is a complex conjugate term. Then, $\tilde{I}_{\mathrm{AC}}(z_{\mathrm{m}},f)(=F\{I_{\mathrm{AC}}(z_{\mathrm{m}},t)\})$ is expressed as

$$\begin{aligned}&\tilde{I}_{\mathrm{AC}}(z_m,f)\\ &\quad\propto\int_{\mathrm{FUT}} dz\cdot F[E_r^*(t)E_S^{'}(z-z_m,t)D(z,t)+c.c.]\\ &\quad=\int_{\mathrm{FUT}} dz\cdot\{\tilde{D}(z,f)\otimes_f\tilde{B}(z-z_m,f)+c.c.\},\end{aligned} \tag{7}$$

where the beat spectrum $\tilde{B}(z-z_{\mathrm{m}},f)$ is defined as

$$\tilde{B}(z-z_m,f)=F\{E_r^*(t)\cdot E'_S(z-z_m,t)\}. \tag{8}$$

Here, $\tilde{B}(z-z_m,f)$ can be expressed as $\tilde{B}(z_m-z,f)$ because it is a function only of the relative distance between z_{m} and z. When sinusoidal modulation is applied to the LD frequency, $\tilde{B}(z-z_m,f)$ is a real function [12], so (7) can be transformed as

$$\begin{aligned}&\tilde{I}_{\mathrm{AC}}(z_m,f)\\ &\quad\propto\int_{\mathrm{FUT}} dz\cdot[\{\tilde{D}(z,f)+\tilde{D}^*(z,f)\}\otimes_f\tilde{B}(z-z_m,f)]\\ &\quad=2\int_{\mathrm{FUT}} dz\cdot[\mathrm{Re}[\tilde{D}(z,f)]\otimes_f\tilde{B}(z_m-z,f)]\end{aligned} \tag{9}$$

In (9), the real part of $\tilde{D}(z,f)$ satisfies

$$\begin{aligned}\mathrm{Re}[\tilde{D}(z,f)]&=\mathrm{Re}\left[\frac{\sqrt{g_{B0}}}{1-j2f/\Delta\nu_B}\right]\\ \propto\mathrm{Re}\left[\frac{1+j2f/\Delta\nu_B}{1+4f^2/\Delta\nu_B^2}\right]&=\frac{1}{1+4f^2/\Delta\nu_B^2}\propto g_B(z,f),\end{aligned} \tag{10}$$

where we define the intrinsic Brillouin gain $g_{\mathrm{B}}(z,f)$ as

$$g_B(z,f)=|\tilde{D}(z,f)|^2=\frac{g_{B0}}{1+4f^2/\Delta\nu_B^2}. \tag{11}$$

Therefore, (9) can be further transformed as

$$\begin{aligned}&\tilde{I}_{\mathrm{AC}}(z_m,f)\\ &\quad\propto\int_{\mathrm{FUT}} dz\cdot[g_B(z,f)\otimes_f\tilde{B}(z_m-z,f)]\\ &\quad=\int_{\mathrm{FUT}} dz\int_{-\infty}^{\infty} df'\cdot g_B(z,f-f')\cdot\tilde{B}(z_m-z,f'),\end{aligned} \tag{12}$$

which leads to the following expression of the effective BGS:

$$\begin{aligned}&\mathrm{BGS}(z_m,f)\\ &\quad=\left|\int_{\mathrm{FUT}} dz\int_{-\infty}^{\infty} df'\cdot g_B(z,f-f')\cdot\tilde{B}(z_m-z,f')\right|^2.\end{aligned} \tag{13}$$

Equation (13) shows that, when the measuring position is z_{m}, the effective BGS is determined by the square of the 2-dimensional convolution of $g_{\mathrm{B}}(z_{\mathrm{m}},f)$ and $\tilde{B}(z_m,f)$. In contrast, in BOCDA, the effective BGS is given by the 2-dimensional convolution of $g_{\mathrm{B}}(z_{\mathrm{m}},f)$ and $|\tilde{B}(z_{\mathrm{m}},f)|^2$ [12]. Although the derivation and the physical picture are different, (13) is similar to that of BOCDA.

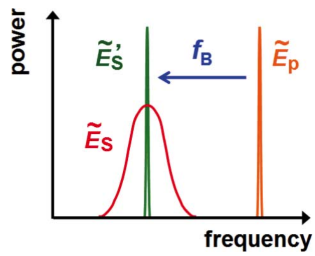

Fig. 4. Definitions of each symbol in (1).

B. Spatial Resolution

Since the effective BGS in BOCDR is determined by the 2-dimensional convolution of the intrinsic Brillouin gain and the beat spectrum as well as in BOCDA, the expression for the spatial resolution in BOCDR can be derived in the same way as that in BOCDA [12].

We need to separate in the cases of fast f_m and slow f_m, where f_m is the modulation frequency of the laser frequency [12]. When f_m is higher than the Brillouin bandwidth $\Delta\nu_\mathrm{B}$, we define the spatial resolution Δz as the distance between the correlation peak and the position where the beat spectrum falls to a half of its peak value. In this case, we estimate only the 0-th component of the beat spectrum, because the other components are outside $\Delta\nu_\mathrm{B}$ [12]. Then we obtain, as in BOCDA [12],

$$\Delta z = \frac{1.52\nu_g}{2\pi\Delta f}, \tag{14}$$

where v_g is the light velocity in the fiber, and Δf is the modulation amplitude of the laser frequency. Thus, when $f_\mathrm{m} > \Delta\nu_\mathrm{B}$, the resolution is in inverse proportion to Δf.

In contrast, when f_m is lower than $\Delta\nu_\mathrm{B}$, we must estimate many components of the beat spectrum within $\Delta\nu_\mathrm{B}$ [12]. We define the spatial resolution Δz as the distance between the correlation peak and the position where the full width of the beat spectrum broadens twice as wide as $\Delta\nu_\mathrm{B}$ [12]. Then we obtain

$$\Delta z = \frac{\nu_g \Delta\nu_B}{2\pi f_m \Delta f}, \tag{15}$$

from which we know that, when $f_\mathrm{m} < \Delta\nu_\mathrm{B}$, the resolution is in inverse proportion not only to Δf but also to f_m. Then, the spatial resolution of BOCDR is given well by the same expression as that of BOCDA. According to (14) and (15), it is clear that f_m higher than $\Delta\nu_\mathrm{B}$ does not contribute to the enhancement of Δz.

When $f_\mathrm{m} = \Delta\nu_\mathrm{B}$, the resolution given by (14) becomes approximately 1.5 times larger than that given by (15). This is valid because the definitions of the resolution for $f_\mathrm{m} > \Delta\nu_\mathrm{B}$ and $f_\mathrm{m} < \Delta\nu_\mathrm{B}$ are the least consistent around $f_\mathrm{m} = \Delta\nu_\mathrm{B}$, where there are several, neither one nor many, components of the beat spectrum within $\Delta\nu_\mathrm{B}$.

V. Limitation of Modulation Amplitude

A. Motivation

The measurement range d_m of BOCDR, which is the distance between the neighboring correlation peaks, is given by [18]

$$d_m = \frac{v_g}{2f_m}. \tag{16}$$

As shown in (15) and (16), there is a trade-off between the measurement range and the spatial resolution, and the ratio of the two values is purely dependent on the modulation amplitude of the laser frequency Δf. Therefore, Δf needs to be increased in order to obtain substantial improvement in the performance of BOCDR. Conventionally, Δf has been limited to a half of the BFS because of the Rayleigh scattering-induced noise, which was also experimentally demonstrated [18], [20].

In this section, however, we theoretically and experimentally show that, by using an FUT shorter than a half of the measurement range, it becomes possible to enhance Δf beyond a half of the BFS.

B. Theory

The electric field of the reference light $E_\mathrm{r}(t)$ at the heterodyne receiver is given as

$$E_r(t) = a_r \exp j\left\{\frac{\Delta f}{f_m}\sin(2\pi f_m t) + \phi(t)\right\}, \tag{17}$$

where a_r is the amplitude, and $\phi(t)$ is the phase noise of the laser. Then, the electric field of the Rayleigh-scattered light $E_\mathrm{R}(t)$ can be expressed as

$$E_R(t) = a_R \exp j\left\{\frac{\Delta f}{f_m}\sin(2\pi f_m t + \varphi) + \phi(t+\tau)\right\}, \tag{18}$$

where a_R is the amplitude, and τ is the time delay; φ is the phase difference of the sinusoidal modulations between the two lightwaves at the heterodyne receiver. While φ becomes 0 at the correlation peaks, φ becomes π at the middle of the intervals of two neighboring correlation peaks $(0 \le \varphi \le \pi)$. Then, the beating noise between the two lightwaves $I_\mathrm{beat}(t)$ can be given as

$$\begin{aligned} I_\mathrm{beat}(t) &= \langle |E_r(t) + E_R(t)|^2 \rangle \\ &= a_r^2 + a_R^2 + 2a_r a_R \\ &\quad \cdot \left\langle \cos\left[\{\phi(t) - \phi(t+\tau)\}\right.\right. \\ &\quad \left.\left. - \frac{2\Delta f}{f_m}\cos\left(2\pi f_m t + \frac{\varphi}{2}\right)\sin\left(\frac{\varphi}{2}\right)\right]\right\rangle. \end{aligned} \tag{19}$$

So, if $\phi(t) - \phi(t+\tau)$ is negligible, the Rayleigh scattering-induced noise spreads from 0 Hz to the following frequency:

$$\begin{aligned} &\max\left[\frac{1}{2\pi}\cdot\frac{\partial}{\partial t}\left\{-\frac{2\Delta f}{f_m}\cos\left(2\pi f_m t + \frac{\varphi}{2}\right)\sin\left(\frac{\varphi}{2}\right)\right\}\right] \\ &= 2\Delta f \cdot \max\left\{\sin\left(2\pi f_m t + \frac{\varphi}{2}\right)\sin\left(\frac{\varphi}{2}\right)\right\} \\ &= 2\Delta f \cdot \max\left\{\sin\left(\frac{\varphi}{2}\right)\right\}, \end{aligned} \tag{20}$$

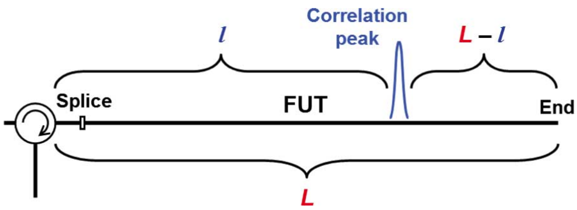

Fig. 5. Definitions of L and l in (21).

which must be lower than the BFS. This means that, if there is no point in the FUT where $\varphi = \pi, \Delta f$ can exceed a half of the BFS. The limitation of Δf is given, by a function not only of BFS but also of measurement range d_{m}, FUT length L, and the distance l between the measuring position and the circulator (See Fig. 5), as

$$\Delta f_{\max} = \frac{\mathrm{BFS}}{2} \cdot \operatorname{cosec}\left\{\frac{\pi \max(L-l, l)}{d_m}\right\}, \tag{21}$$

where, of $L-l$ and l, the larger length contributes to the limitation of Δf. When a distributed measurement is performed, the measuring position must be scanned along the whole length of the FUT. Therefore, $\Delta f_{\max}$ as a sensing system is given by

$$\Delta f_{\max} = \frac{\mathrm{BFS}}{2} \cdot \operatorname{cosec}\left(\frac{\pi L}{d_m}\right), \tag{22}$$

which means that we can enhance Δf beyond a half of the BFS by using an FUT shorter than a half of the measurement range.

C. Experimental Verification

The experimental setup to verify (21) is the same as that reported previously [18], [19]. Using a 100-m FUT ($L = 100$ m), the modulation frequency f_{m} was set to 286.90 kHz, which corresponds to $d_{\mathrm{m}} = 349.2$ m and $l = 1$ m. Fig. 6(a) shows the measured whole spectra of the electrical output when Δf was increased from 0.1 GHz. As Δf became larger, the Rayleigh scattering-induced noise spread from 0 Hz. When the noise began to overlap the BGS peak at about 10.85 GHz, Δf was about 6.9 GHz as shown in Fig. 6(b), which is the optical spectrum of the reference light after passing the optical filter. The spectrum is slightly assymetric due to the dependence of the LD output on injection current. According to (21), the theoretical limitation of Δf is calculated to be 6.98 GHz, which is in good agreement with the experimental result.

The same experiment was also performed when $f_{\mathrm{m}} = 296.17$ kHz, $d_{\mathrm{m}} = 338.3$ m, $L = 100$ m, and $l = 80$ m. The experimental results shown in Figs. 7(a) and (b) indicate that the limitation of Δf was about 7.95 GHz. This is in good agreement with the theoretical value of 8.01 GHz. The slight discrepancy seems to originate from the assumption that the time dependence of the phase noise, that is, the linewidth of the light source, is negligible in deriving (21).

According to (15), either f_{m} or Δf must be increased to enhance the resolution. In [20], by setting $f_{\mathrm{m}} = \Delta\nu_{\mathrm{B}}$ and Δf to a half of the BFS, 6-mm resolution was obtained using a tellurite glass fiber. So the fact that Δf can be higher than a half of the BFS indicates that the spatial resolution even higher than 6 mm is feasible in BOCDR. This kind of usage, however, is not beneficial from the viewpoint of the effective number of sensing points. In order to enhance the measurement range substantially, we need to employ either a temporal gating scheme [21] or a double-modulation scheme [22].

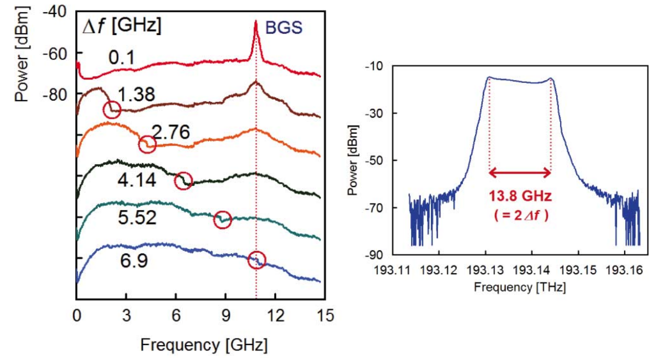

(a) (b)

Fig. 6. (a) Measured electrical spectra when Δf was increased from 0.1 to 6.9 GHz. Each spectrum is shifted by 20 dB. The values on the ordinate are valid only for $\Delta f = 0.1$ GHz. (b) Measured optical spectrum of the reference light after passing the optical filter.

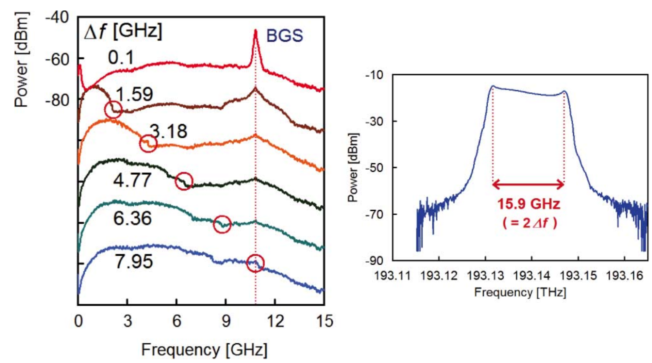

(a) (b)

Fig. 7. (a) Measured electrical spectra when Δf was increased from 0.1 to 7.95 GHz. Each spectrum is shifted by 20 dB. The values on the ordinate are valid only for $\Delta f = 0.1$ GHz. (b) Measured optical spectrum of the reference light after passing the optical filter.

VI. Conclusion

We theoretically and experimentally analyzed the operation of BOCDR. First, we clarified that BOCDR is not based on SBS but on spontaneous Brillouin scattering. Next, we showed that the effective BGS in BOCDR is given by the 2-dimensional convolution of the intrinsic Brillouin gain and the beat spectrum. Although the derivation and the physical picture are different, this expression is almost the same as that of BOCDA. Then, we derived the expression for the spatial resolution of BOCDR, which was the same as that of BOCDA. Finally, we demonstrated that the modulation amplitude of the laser frequency, which determines the spatial resolution, can be enhanced beyond the conventional limitation of a half of the BFS by employing an FUT shorter than a half of the measurement range. We believe that the presented results improve our understanding of BOCDR, and provide helpful guidelines for its practical use in smart materials and structures.

APPENDIX

We verify (1) and (2) when the linewidth of the pump light is 0. When f_P is the frequency of the pump light, $\tilde{E}_\mathrm{P}(z,f)$ is expressed as

$$\tilde{E}_p(z,f) = \delta[f - f_p], \tag{A1}$$

where the amplitude was normalized. Then, $\tilde{E}_\mathrm{S}(z - z_\mathrm{m}, f')$ can be calculated, using (1) and (2), as

$$\begin{aligned}
&\tilde{E}_S(z - z_m, f') \\
&\quad = \delta[f + f_B(z) - f_p] \otimes_f D(z,f) \\
&\quad = \int_{-\infty}^{\infty} df \cdot \delta[f + f_B(z) - f_p] \cdot \tilde{D}(z, f' - f) \\
&\quad = \tilde{D}(z, f' - f_p + f_B(z)) \\
&\quad = \frac{g_{B0}^{1/2}}{1 - j2(f' - f_p + f_B(z))/\Delta\nu_B} \\
&\quad = \frac{g_{B0}^{1/2}}{1 - j2(f' - (f_p + f_B(z)))/\Delta\nu_B},
\end{aligned} \tag{A2}$$

which is the correct expression for $\tilde{E}_\mathrm{S}(z - z_\mathrm{m}, f')$.

REFERENCES

[1] T. Kurashima, T. Horiguchi, H. Izumita, S. Furukawa, and Y. Koyamada, "Brillouin optical-fiber time domain reflectometry," *IEICE Trans. Commun.*, vol. E76-B, pp. 382–390, 1993.

[2] K. Shimizu, T. Horiguchi, Y. Koyamada, and T. Kurashima, "Coherent self-heterodyne Brillouin OTDR for measurement of Brillouin frequency shift distribution in optical fibers," *J. Lightw. Technol.*, vol. 12, no. 5, pp. 730–736, May 1994.

[3] M. N. Alahbabi, Y. T. Cho, and T. P. Newson, "150-km-range distributed temperature sensor based on coherent detection of spontaneous Brillouin backscatter and in-line raman amplification," *J. Opt. Soc. Amer. B*, vol. 22, pp. 1321–1324, 2005.

[4] M. A. Soto, G. Bolognini, and F. D. Pasquale, "Analysis of optical pulse coding in spontaneous Brillouin-based distributed temperature sensors," *Opt. Exp.*, vol. 16, pp. 19097–19111, 2008.

[5] T. Horiguchi and M. Tateda, "BOTDA—Nondestructive measurement of single-mode optical fiber attenuation characteristics using Brillouin interaction: Theory," *J. Lightw. Technol.*, vol. 7, no. 5, pp. 1170–1176, May 1989.

[6] T. Horiguchi, K. Shimizu, T. Kurashima, M. Tateda, and Y. Koyamada, "Development of a distributed sensing technique using Brillouin scattering," *J. Lightw. Technol.*, vol. 13, no. 7, pp. 1296–1302, Jul. 1995.

[7] A. Vedadi, D. Alasia, E. Lantz, H. Maillotte, L. Thevenaz, M. Gonzalez-Herraez, and T. Sylvestre, "Brillouin optical time-domain analysis of fiber-optic parametric amplifiers," *IEEE Photon. Technol. Lett.*, vol. 19, pp. 179–181, 2007.

[8] W. Li, X. Bao, Y. Li, and L. Chen, "Differential pulse-width pair BOTDA for high spatial resolution sensing," *Opt. Exp.*, vol. 16, pp. 21616–21625, 2008.

[9] A. W. Brown, B. G. Colpitts, and K. Brown, "Dark-pulse Brillouin optical time-domain sensor with 20-mm spatial resolution," *J. Lightw. Technol.*, vol. 25, no. 1, pp. 381–386, Jan. 2007.

[10] T. Sperber, A. Eyal, M. Tur, and L. Thevenaz, "High spatial resolution distributed sensing in optical fibers by Brillouin gain-profile tracing," *Opt. Exp.*, vol. 18, pp. 8671–8679, 2010.

[11] K. Y. Song and H. J. Yoon, "High-resolution Brillouin optical time domain analysis based on Brillouin dynamic grating," *Opt. Lett.*, vol. 35, pp. 52–54, 2010.

[12] K. Hotate and T. Hasegawa, "Measurement of Brillouin gain spectrum distribution along an optical fiber using a correlation-based technique—Proposal, experiment and simulation," *IEICE Trans. Electron.*, vol. E83-C, pp. 405–412, 2000.

[13] K. Hotate and M. Tanaka, "Distributed fiber Brillouin strain sensing with 1-cm spatial resolution by correlation-based continuous-wave technique," *IEEE Photon. Technol. Lett.*, vol. 14, no. 2, pp. 179–181, Feb. 2002.

[14] K. Y. Song, Z. He, and K. Hotate, "Distributed strain measurement with millimeter-order spatial resolution based on Brillouin optical correlation domain analysis," *Opt. Lett.*, vol. 31, pp. 2526–2528, 2006.

[15] K. Y. Song and K. Hotate, "Brillouin optical correlation domain analysis in linear configuration," *IEEE Photon. Technol. Lett.*, vol. 20, no. 24, pp. 2150–2152, Dec. 2008.

[16] A. Fellay, L. Thevenez, M. Facchini, M. Nikles, and P. Robert, "Distributed sensing using stimulated Brillouin scattering: Towards ultimate resolution," *Tech. Dig. Opt. Fiber Sens.*, vol. 16, pp. 324–327, 1997.

[17] H. Naruse and M. Tateda, "Trade-off between the spatial and the frequency resolutions in measuring the power spectrum of the Brillouin backscattered light in an optical fiber," *Appl. Opt.*, vol. 38, pp. 6516–6521, 1999.

[18] Y. Mizuno, W. Zou, Z. He, and K. Hotate, "Proposal of Brillouin optical correlation-domain reflectometry (BOCDR)," *Opt. Exp.*, vol. 16, pp. 12148–12153, 2008.

[19] Y. Mizuno, Z. He, and K. Hotate, "One-end-access high-speed distributed strain measurement with 13-mm spatial resolution based on Brillouin optical correlation-domain reflectometry," *IEEE Photon. Technol. Lett.*, vol. 21, no. 7, pp. 474–476, Apr. 2009.

[20] Y. Mizuno, Z. He, and K. Hotate, "Distributed strain measurement using a tellurite glass fiber with Brillouin optical correlation-domain reflectometry," *Opt. Commun.*, vol. 283, pp. 2438–2441, 2010.

[21] Y. Mizuno, Z. He, and K. Hotate, "Measurement range enlargement in Brillouin optical correlation-domain reflectometry based on temporal gating scheme," *Opt. Exp.*, vol. 17, pp. 9040–9046, 2009.

[22] Y. Mizuno, Z. He, and K. Hotate, "Measurement range enlargement in Brillouin optical correlation-domain reflectometry based on double-modulation scheme," *Opt. Exp.*, vol. 18, pp. 5926–5933, 2010.

Yosuke Mizuno was born in Hyogo, Japan, on October 13, 1982. He received the B.E., M.E., and Dr. Eng. degrees in electronic engineering from the University of Tokyo, Japan, in 2005, 2007, and 2010, respectively.

In 2004, he worked on optical information processing at the University of Tokyo. From 2005 to 2007, he was engaged in spin- electronics, and studied spin hot-carrier transistors for his master degree. Since 2007, he had been working on Brillouin optical correlation-domain reflectometry for his Dr. Eng. at the University of Tokyo. From 2007 to 2010, he was a Research Fellow, DC1, of the Japan Society for the Promotion of Science (JSPS). In 2010, he became a Postdoctoral Research Fellow of Tokyo Institute of Technology, Kanagawa, Japan. He is currently a Research Fellow, PD, of JSPS. His research interests include fiber-optic sensors, polymer optics, and ultrasonics.

Dr. Mizuno is a member of the Japanese Society of Applied Physics (JSAP), and the Institute of Electronics, Information, and Communication Engineers (IEICE) of Japan.

Weiwen Zou (S'05-M'08) was born in Jiangxi, China, on January 3, 1981. He received the B.S. degree in physics and the M.S. degree in optics from Shanghai Jiao Tong University, China, in 2002 and 2005, respectively, and the Dr. Eng. degree in optoelectronics from the University of Tokyo, Japan, in 2008.

In 2003, he was engaged in research of non-volatile photorefractive-based holography at University of Electro-Communications, Japan, as an exchange student. Since 2005, he had been working on Brillouin-scattering-based discriminative sensing of strain and temperature for his doctoral research in electronic engineering, the University of Tokyo, Japan. From 2008 to 2009, he was a Postdoctoral Research Fellow at the University of Tokyo. In 2009, he became a Project Assistant Professor of the University of Tokyo. In 2010, he joined Shanghai Jiao Tong University as an Associate Professor. His current research interests include fiber-optic distributed sensors, fiber-optic measurement and optical information processing.

Dr. Zou is a member of the Optical Society of America (OSA).

Zuyuan He (M'00) received the B.S. and M.S. degrees in electronic engineering from Shanghai Jiao Tong University, Shanghai, China, in 1984 and 1987, respectively, and the Dr. Eng. degree in optoelectronics from the University of Tokyo, Tokyo, Japan, in 1999.

He joined Nanjing University of Science and Technology, Nanjing, China as a Research Associate in 1987, and became a Lecturer in 1990. From 1995 to 1996, he was a Research Fellow in the Research Center for Advanced Science and Technology (RCAST), the University of Tokyo. In 1999, he became a Research Associate of the University of Tokyo, where he worked on measurement and characterization of fiber optic components and systems, fiber optic reflectometry, fiber optic sensors, and multi-dimensional optical information processing. In 2001, he joined CIENA Corporation, Linthicum, Maryland, USA, as a Lead Engineer responsible for optical testing and optical process development. He returned to the University of Tokyo as a Lecturer in 2003, and became an Associate Professor in 2005. He is now a Professor at the Center of Excellence (COE) in Electrical and Electronic Engineering, the University of Tokyo. His current research interests include optical fiber sensors, optical fiber measurement, and optical information processing.

Prof. He is a member of the Optical Society of America (OSA), and a member of the Institute of Electronics, Information, and Communication Engineers (IEICE) of Japan.

Kazuo Hotate (M'91–SM'98–F'03) was born in Tokyo, Japan, on June 20, 1951. He received the B.E., M.E., and Dr. Eng. degrees in electronic engineering from the University of Tokyo, Tokyo, Japan, in 1974, 1976, and 1979, respectively.

In 1979, he joined the University of Tokyo as a Lecturer. He became a Professor in 1993 at the Research Center for Advanced Science and Technology (RCAST), the University of Tokyo. Currently, he is a Professor in the Department of Electrical Engineering and Information Systems, School of Engineering, the University of Tokyo. He served as the Dean of Faculty and Graduate School of Engineering, the University of Tokyo in 2008 and 2009. He was engaged in projection-type holography, measurement and analysis of optical fiber characteristics. At present, he is working on photonic sensing. He has authored and coauthored several books on optical fibers and optical fiber sensors and more than 370 journal papers and international conference presentations.

Prof. Hotate is a Fellow of IEEE, a Fellow of Institute of Electronics, Information, and Communication Engineers (IEICE), a Fellow of Society of Instrumentation and Control Engineers (SICE), and a Fellow of Japan Society of Applied Physics (JSAP). He received academic awards, such as SPIE DSS Life-Time Achievement Award, Ichimura Prize, and Hasunuma Prize (SICE). He was a BoG member of IEEE Photonic Society. He served as the co-chairs for SPIE Fiber Optic Gyros: Twentieth Anniversary Conference (1996), the Technical Program Committee Chair for the 13th International Conference on Optical Fiber Sensors (OFS-13) (1999), and the General Chair for OFS-16 (2003).